Available online at www.sciencedirect.com

SciVerse ScienceDirect

Journal of the European Ceramic Society 32 (2012) 1117–1135

www.elsevier.com/locate/jeurceramsoc

Thermodynamic approach to the vaporization and growth phenomena of SiC ceramics. I. SiC and $SiC–SiO_2$ mixtures under neutral conditions

G. Honstein, C. Chatillon *, F. Baillet

Science et Ingénierie des Matériaux et Procédés (SIMAP associated with CNRS-UMR 5466, UJF/INP-Grenoble) Domaine Universitaire, BP 75, 38402 - Saint Martin d'Hères, France

Available online 17 December 2011

Abstract

Matter transport by vaporization and condensation processes during sintering or consolidation of SiC components at high temperature is analysed using thermodynamics of the binary Si–C and ternary Si–C–O systems. The erosion flows due to vaporization and the potential growth flow of SiC are calculated in order to determine the conditions prevailing at the surface of SiC powder grains. Pure SiC vaporization leads to rapid precipitation of carbon at the SiC surface. Vaporization of $SiC–SiO_2$ mixtures under neutral atmospheric conditions or absolute vacuum contributes to the rapid departure of any Si or C impurities first of all, and then silica according to congruent vaporization in the $SiC–SiO_2$ pseudo-binary system. The calculated SiC growth rate by vapour transport is always less than the erosion rate and further subsequent growth of pure SiC cannot be obtained as long as silica co-exists with SiC.

© 2011 Elsevier Ltd. All rights reserved.

Keywords: Thermodynamics; SiC; $SiC–SiO_2$; High temperature vaporization; Growth

1. Introduction

In this study, a theoretical approach based on thermodynamics is used to describe the complex vaporization and reverse condensation phenomena in Si–C binary and Si–C–O ternary systems. As SiC-based ceramics often have to be manufactured at high temperatures, vaporization occurs and interferes with the growth and densification processes. This interference can have both a positive, desirable influence on the manufacturing process as well as a negative effect. For instance, gas-phase material transport in the components leads to structural bonding, while the same transport process can also deposit material outside the components and lead to premature ageing of kiln equipment. Obtaining more information on gas-phase behaviour as well as vaporization phenomena during the manufacturing process would help to improve the quality of the material produced in terms of densification or mechanical consolidation and prevent premature ageing of the kiln equipment.

Because of their refractory properties, SiC-based ceramics are also gaining increasing importance in high temperature applications. It is therefore important to have a detailed understanding of their evaporation behaviour, the final composition limits and potential improvement possibilities. Our analysis also considered the Si–C–O ternary system because it is important to know the vaporization phenomena of the mixture of SiC with SiO_2 since silica is always present as a native layer on the open surface of silicon-based materials and silica is sometimes used as an additive with other oxides.

Part I of this article deals with "pure" Si–C or Si–C–O systems, *i.e.*, considering their vaporization processes without any interference either from atmospheric contamination (mainly oxygen) or from the containers. Part II analyses the influence of oxygen on the SiC surface state, *i.e.*, the influence of so-called active or passive oxidation of SiC on the surface chemical state and transport processes.

2. Main basic features of the Si–C and Si–C–O phase diagrams

2.1. Si–C phase diagram

The only compound found in the Si–C binary system is SiC and the phase diagram was originally compiled from experimental data by Olesinski and Abbaschian[1] in 1984. The proposed phase diagram is based on the peritectic temperature determined

* Corresponding author. Tel.: +33 0476 82 65 11; fax: +33 0476 82 67 67.
E-mail address: christian.chatillon@simap.inp-grenoble.fr (C. Chatillon).

0955-2219/$ – see front matter © 2011 Elsevier Ltd. All rights reserved.
doi:10.1016/j.jeurceramsoc.2011.11.032

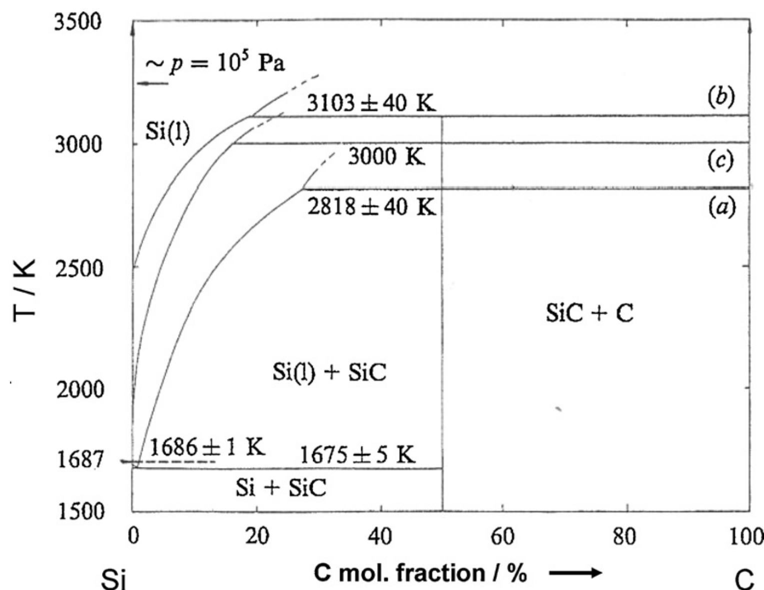

Fig. 1. Different Si–C phase diagrams as presented in literature. (a) As retained by Olesinski and Abbaschian,[1] (b) as retained by Gröbner et al.[5] and SGTE,[6] and (c) early calculated by Kaufman.[7]

by Dolloff[2] which is compatible with large C solubility along the liquidus and at the eutectic point. Discrepancies in eutectic and peritectic temperatures as well as in C solubility in Si liquid could not be explained at that time. Furthermore, based on (i) new determinations confirming the lower C solubility data in liquid silicon as determined by Kleykamp and Schumacher[3] and as retained in a recent compilation by Durand and Duby[4] and (ii) new eutectic temperatures experimentally measured by direct reference to pure Si melting, Gröbner et al.[5] pointed out that the best agreement between experimental data imposes a peritectic temperature of about 3100 K with C mole fraction in the liquid phase equal to ≈18%, and an eutectic temperature of 1686 K with a very low C solubility equal to 0.02 at%, as shown in Fig. 1.

The latter value was chosen here, as retained by STGE[6] in agreement with Gröbner et al.,[5] *i.e.*, a lower solubility in the liquid phase and a peritectic temperature of 3103 K, in agreement with original work by Scace and Slack.[8] Consequently, any thermodynamic calculations of vaporization processes can be performed up to 2500 K assuming a silicon activity equal to 1 for the Si–SiC two-phase domain. The effective small departure of silicon activity from unity had previously been confirmed by Chatillon[9] and Rocabois et al.[10] using mass spectrometry.

2.2. Si–C–O phase diagram

The Si–C–O ternary phase diagram is of great interest to all those who work with SiC because of the unavoidable presence of silicon oxide due to the oxidation of at least the silicon surface sites exposed to oxygen-containing atmospheres. Ghosh and St-Pierre[11] calculated the Si–C–O phase diagram under one atmosphere at 1700 K. Two line compounds SiC and SiO_2 exist and in their pseudobinary section no reciprocal solubility is known, and no ternary compound exists at equilibrium although some intermediate phases have been observed by different authors:

- Pampuch et al.,[12] after moderate oxidation of SiC, observed by photoelectron spectroscopy (XPS) some peaks attributed to O–Si–C bonds and proposed a phase with a mean composition of around $Si_2O_2C_2$.
- Porte and Sartre,[13] from XPS measurements on Nicalon fibres, observed a surface rich in oxygen and depleted in silicon. The peaks revealed a new bond in addition to the known Si–O and Si–C bonds. The new bond would be attributed to SiO_x and they propose a new compound SiO_xC_y.
- Nagamori et al.[14] performed a thermodynamic analysis of the stability of Nicalon fibres as an amorphous and stable phase with composition $SiC_\alpha O_\beta$ which would co-exists with SiO_2 and C. The mean proposed composition corresponds to $Si_5C_6O_2$. The thermodynamic cycles used suffer from a lack of thermodynamic data and from the uncertainties associated with the necessary estimates of certain thermodynamic properties.
- Vargas et al.[15] recently presented SiCO-like amorphous compounds as structures formed by nano-domains with special graphene (basal graphite planes) walls. Calorimetric measurements of these amorphous phases referred experimentally to the pure SiO_2, SiC and graphite compounds showed negative enthalpies of formation which became more pronounced with C enrichment. The stability of the different Si–C and Si–O chemical bonds around the same carbon as well as the nano-domain structure could explain the apparent stability of these mixtures of phases against re-crystallisation at high temperature, *i.e.*, the existence of a rather high kinetic enthalpy barrier that prevents re-crystallization into separate phases SiC and SiO_2.

According to the experimental vaporization work by mass spectrometry of Rocabois et al.[16–18] and Chatillon et al.[19] the vaporization of silicon monoxide or carboxides (also called "Black Glasses") is associated with low evaporation coefficients and consequently leads to determined SiO or CO vapour pressures lower than expected at equilibrium due to a kinetic barrier. These low vapour pressure values act as artefacts that, when introduced in thermodynamic cycles, tended to decrease some Gibbs enthalpies and consequently to apparently prove the existence of stable compounds. Moreover, when using the determined evaporation coefficients to recalculate the real equilibrium pressures that should be established in effusion cells from the measured ones, Rocabois et al.[16] showed, for instance, that equilibrium partial pressures over SiO(amorphous) are not different from those over Si(s) + SiO_2(s) mixtures. For these reasons, in the present work the proposed ternary compounds are considered to be only metastable compounds obtained in specific constrained and growth structures such as, for instance, in oxidation growth layers or in fibres. Consequently, these compounds are not taken into account in our subsequent calculations.

The present calculations are normally performed using complex equilibrium software such as Thermocalc,[20] Thermosuite[21] or FactSage,[22] etc. . . However, the conventional thermodynamic calculations – that have to be performed in well-defined conditions, such as homogeneous temperature and constant total applied pressure – cannot manage directly the whole set of matter flows at the surface of SiC grains because the present thermodynamic calculations should be associated with matter flow regimes, such as molecular flows under vacuum, viscous (laminar or convective) flows under carrier gas with some gas diffusion in a boundary layer, in order to solve the complete mechanisms involved in experiments or industrial furnaces. In the present work, attention is focused on local chemical conditions prevailing at the surface of any SiC grain in order to understand the important mechanisms that explain, at the same time, both the erosion and the growth of these grains. These local conditions are believed to be the main constraints governing SiC erosion or growth. Thus, the following set of calculations could be performed with usual software only when associated with sub-routines capable of managing the flow balance constraints, as already conducted by Heyrman et al.[23,24] using the Parrot module of Thermocalc in the case of congruent vaporizations.

3. Vaporization behaviour in the Si–C binary system

3.1. Vaporization in the Si–C binary system

Vaporization of pure SiC, which is known to have a very restricted non-stoichiometric domain not strictly described by thermodynamics up till now, comes within two two-phase (or diphasic) domains Si–SiC and SiC–C. The gaseous phase contains atomic Si(g) and C(g) and a number of molecules which were studied using high temperature mass spectrometry (HTMS) or Knudsen cell mass spectrometry (KCMS). The most important gaseous species are Si, Si_2, Si_3, Si_2C, SiC_2, C_3, C_5 and C and these gaseous species are tabulated in the JANAF thermochemical tables.[25] Minor gaseous species, *i.e.*, less than 1% in the vapour phase not taken into account in the present work are Si_4 to Si_8, C_2 and the gaseous carbides SiC, Si_2C_2, Si_2C_3, Si_3C_2 Si_3C, Si_4C as evidenced by high temperature mass spectrometry.[9,26–31] These minor species – except SiC(g) which is tabulated in JANAF tables – will not be taken into account in the present work.

The vapour pressures in equilibrium with SiC can be calculated from the following elementary independent reactions as for instance:

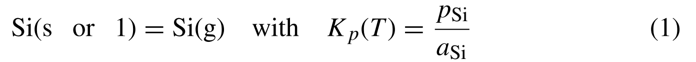

$$\mathrm{Si(s\quad or\quad 1) = Si(g)} \quad \text{with} \quad K_p(T) = \frac{p_{\mathrm{Si}}}{a_{\mathrm{Si}}} \tag{1}$$

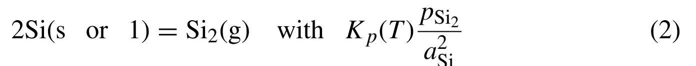

$$\mathrm{2Si(s\quad or\quad 1) = Si_2(g)} \quad \text{with} \quad K_p(T)\frac{p_{\mathrm{Si_2}}}{a_{\mathrm{Si}}^2} \tag{2}$$

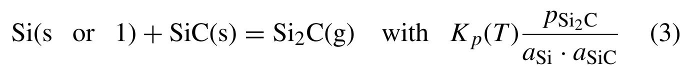

$$\mathrm{Si(s\quad or\quad 1) + SiC(s) = Si_2C(g)} \quad \text{with} \quad K_p(T)\frac{p_{\mathrm{Si_2C}}}{a_{\mathrm{Si}} \cdot a_{\mathrm{SiC}}} \tag{3}$$

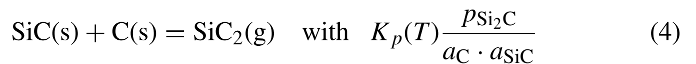

$$\mathrm{SiC(s) + C(s) = SiC_2(g)} \quad \text{with} \quad K_p(T)\frac{p_{\mathrm{Si_2C}}}{a_{\mathrm{C}} \cdot a_{\mathrm{SiC}}} \tag{4}$$

The activities of pure solids are equal to 1 by definition, and is the same for liquid Si as it is known that carbon solubility remains very low at least up to 2500 K. Partial pressures are calculated from JANAF tables[25] for the main vapour species in the two two-phase domains Si–SiC and SiC–C and presented in Fig. 2 for SiC with excess silicon. The behaviour of the vapour pressures in this two-phase system can be plotted according to the general thermodynamics relation $\log p = A/T + B$. Coefficients A and B are listed in Table 1. For two-phase SiC–C, the results of the calculation are shown in Fig. 3 and coefficients A and B are also listed in Table 1.

3.2. Evaporation flows in the Si–C binary system

Using the plots of partial pressures in equilibrium with a chosen binary composition, the composition of the gaseous phase can now be obtained in terms of mole number of each component and then compared to the composition of the condensed phase. The following equations were used to calculate the composition of the gaseous phase applying the perfect gas law for unit volume V:

$$N_{\mathrm{Si}} = \frac{RT}{V}[p_{\mathrm{Si}} + 2p_{\mathrm{Si_2}} + 3p_{\mathrm{Si_3}} + p_{\mathrm{SiC_2}} + p_{\mathrm{Si_2C}} + p_{\mathrm{SiC}} + \cdots] \tag{5}$$

$$N_{\mathrm{C}} = \frac{RT}{V}[p_{\mathrm{C}} + 3p_{\mathrm{C_3}} + 2p_{\mathrm{SiC_2}} + p_{\mathrm{Si_2C}} + p_{\mathrm{SiC}} + \cdots] \tag{6}$$

and then the mole fraction in the vapour phase:

$$X_{\mathrm{Si}} = \frac{N_{\mathrm{Si}}}{N_{\mathrm{Si}} + N_{\mathrm{C}}} \tag{7}$$

$$X_{\mathrm{C}} = \frac{N_{\mathrm{C}}}{N_{\mathrm{Si}} + N_{\mathrm{C}}} \tag{8}$$

The ratio $X_{\mathrm{Si}}/X_{\mathrm{C}} = N_{\mathrm{Si}}/N_{\mathrm{C}}$ for the gas phase is displayed in Fig. 4 with full black symbols for the two diphasic systems rich in Si and rich in C. This figure shows that the gaseous phase always

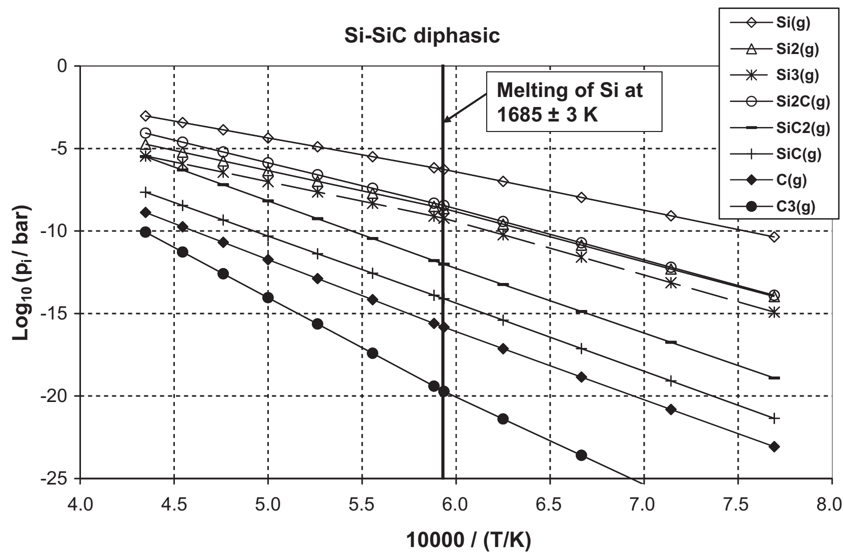

Fig. 2. Partial vapour pressures above pure SiC with excess of Si calculated from JANAF tables.[25]

contains more silicon than carbon compared to the pure SiC compound (ratio = 1:1) regardless of the composition of the paired two-phase mixtures (dilute solutions based on either pure Si or pure C are not considered because these solutions are not known and their composition range is probably very limited). In the case of any pure SiC or diphasics based on SiC vaporization under neutral gas atmosphere, the mass loss will be proportional to the number of moles $N(i)$ multiplied by the carrier gas (slow) flow rate. So, an original pure SiC non-stoichiometric compound in a closed vessel or in a neutral gas flow (low flow rate in order to obtain a saturated vapour) will lose Si in excess and will turn into a two-phase SiC–C component: a carbon residue will necessarily form by precipitation at the surface. This behaviour has already been frequently observed by numerous researchers working on this system. The C atoms appear rapidly at the surface even at low temperature (≈1100 K) as observed by Muehlhoff et al.[32] using Auger electron spectroscopy and this C surface precipitate will re-crystallize rapidly into graphite as observed by Behrens and Rinehart[33] using X-Ray diffraction methods.

Table 1
A and *B* coefficients for the decimal logarithmic plot of partial pressures in equilibrium with the two two-phase domains each side of SiC as an inverse function of temperature, $\log_{10}(p/\text{bar}) = A/(T/\text{K}) + B$. Note that the slope changes because of Si melting at 1685 K.

Gaseous species over the Si–C system phases	*A*		*B*	
Two-phase Si–SiC	$T < 1685$ K[a]	$T > 1685$ K[a]	$T < 1685$ K[a]	$T > 1685$ K[a]
Si	−23,293.8	−20,436.0	7.55862	5.85968
Si_2	−30,336.6	−24,622.0	9.36871	5.97244
Si_3	−32,429.3	−23,747.3	10.02829	4.86736
Si_2C	−31,024.6	−27,654.5	9.96267	7.95579
SiC_2	−39,194.0	−41,143.1	11.24645	12.39919
SiC[b]	−41,219.0	−40,713.7	10.35525	10.05192
C	−41,235.1	−43,825.7	8.64198	10.18002
C_3	−53,016.1	−60,787.8	11.74281	16.35693
Two-phase SiC–C				
Si	−27,022.3	−26,752.3	7.96735	7.80445
Si_2	−37,793.8	−37,254.6	10.18617	9.86198
Si_3	−43,615.1	−42,696.2	11.25449	10.70167
Si_2C	−34,753.2	−33,970.8	10.37140	9.90056
SiC_2	−35,465.4	−34,826.8	10.83772	10.45442
SiC[b]	−41,219.0	−40,713.7	10.35525	10.05192
C	−37,506.6	−37,509.4	8.2335.5	8.23525
C_3	−41,830.4	−41,838.9	10.51662	10.52262
Activity of Si	−3720.4	−63,16.3	0.40280	1.94477

Data for calculations are taken from JANAF tables.[25]
[a] This temperature is the melting temperature of pure silicon.
[b] The SiC partial pressure over the two two-phase domains is the same since the same equilibrium is considered: SiC(s) = SiC(g).

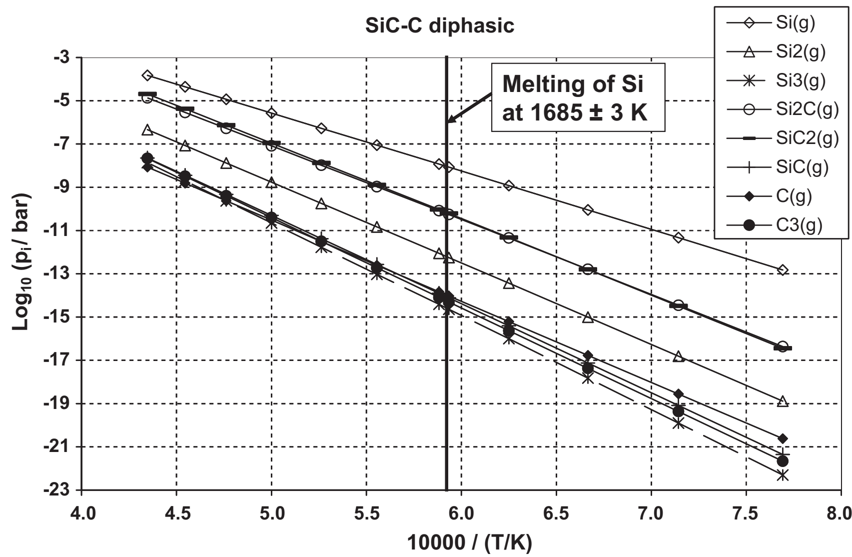

Fig. 3. Partial vapour pressures above pure SiC with excess of C calculated from JANAF tables.[25]

In the case of vaporization under molecular regime (rarefied vacuum), it is the composition of the vaporized atomic flows (Knudsen flows at the surface or at any orifice of a container) that counts rather than the composition of the vapour pressure since the mass loss is directly related to the flow composition. During mass spectrometric experiments using effusion cells, the Knudsen flows are indeed observed. Thus, relations (9) and (10) are used to calculate the atomic flow of Si and C per unit time for a vaporization surface S:

$$F_{\mathrm{Si}} = \frac{S}{\sqrt{2\pi RT}}\left[\frac{p_{\mathrm{Si}}}{\sqrt{M_{\mathrm{Si}}}} + \frac{2p_{\mathrm{Si_2}}}{\sqrt{2M_{\mathrm{Si}}}} + \frac{3p_{\mathrm{Si_3}}}{\sqrt{3M_{\mathrm{Si}}}} + \frac{2p_{\mathrm{Si_2C}}}{\sqrt{2M_{\mathrm{Si}}+M_{\mathrm{C}}}} + \frac{p_{\mathrm{SiC_2}}}{\sqrt{M_{\mathrm{Si}}+2M_{\mathrm{C}}}} + \frac{p_{\mathrm{SiC}}}{\sqrt{M_{\mathrm{Si}}+M_{\mathrm{C}}}}\right] \quad (9)$$

$$F_{\mathrm{C}} = \frac{S}{\sqrt{2\pi RT}}\left[\frac{p_{\mathrm{C}}}{\sqrt{M_{\mathrm{C}}}} + \frac{3p_{\mathrm{C_3}}}{\sqrt{3M_{\mathrm{C}}}} + \frac{p_{\mathrm{Si_2C}}}{\sqrt{3M_{\mathrm{Si}}+M_{\mathrm{C}}}} + \frac{2p_{\mathrm{SiC_2}}}{\sqrt{M_{\mathrm{Si}}+2M_{\mathrm{C}}}} + \frac{p_{\mathrm{Sic}}}{\sqrt{M_{\mathrm{Si}}+M_{\mathrm{C}}}}\right] \quad (10)$$

The $F_{\mathrm{Si}}/F_{\mathrm{C}}$ ratio must then be compared to the composition ratio $X_{\mathrm{Si}}/X_{\mathrm{C}} = 1$ of the solid SiC phase. The presence of the molar masses in these flow expressions leads to a slightly, but significant, difference in gas composition ratios under molecular flow compared to those calculated for transport by carrier gas atmospheres (slow viscous flow) as shown in Fig. 4. During the spectrometric measurements particular attention must be paid to this difference due to vacuum evaporation processes. Moreover, when any flow condition is established that sweeps out all gases

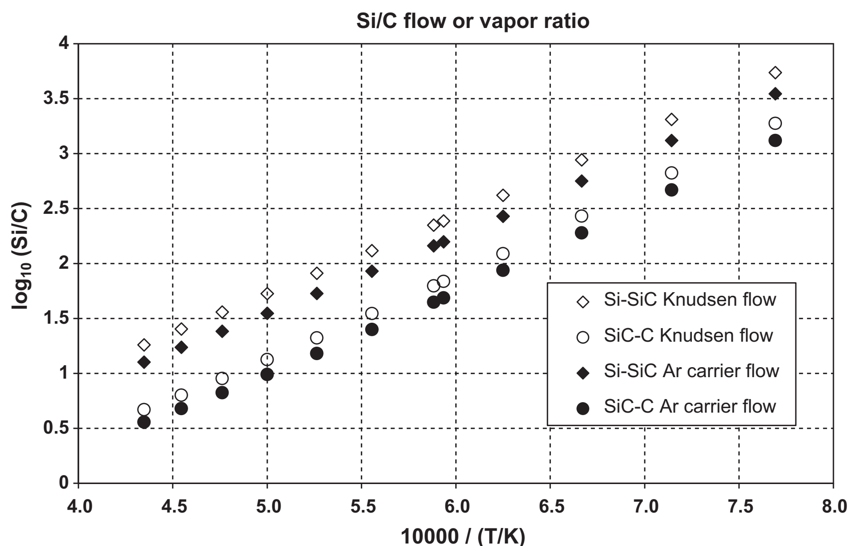

Fig. 4. Decimal logarithm of the gaseous molar fraction ratio $X_{\mathrm{Si}}/X_{\mathrm{C}} = N_{\mathrm{Si}}/N_{\mathrm{C}}$ (viscous flow as Ar carrier gas flow) for SiC rich in Si and for SiC rich in C and comparison with the molecular (Knudsen) flow composition $F_{\mathrm{Si}}/F_{\mathrm{C}}$ in vacuum vaporization.

at the surface, it is this Knudsen condition that gives the real maximum available evaporation flow as used, for instance, by Nickel et al.[34] in their calculations for active oxidation of SiC.

3.3. Vaporization of the SiC compound

Regarding the SiC compound behaviour itself, the aim is to determine what happens between the two diphasic domains when an excess of silicon is lost by vaporization. The components Si and C can be considered in the non-stoichiometric Si_xC_y compound as a solid solution (s, s) according to the equilibrium (x and y being close to 1):

$$Si_xC_y = x\text{Si(s, s in SiC)} + y\text{C(s, s in SiC)} \quad \text{with}$$

$$K_p(T) = \frac{a_{Si} \cdot a_C}{a_{SiC}} \qquad (11)$$

The equilibrium constant is calculated from the standard free enthalpies listed in the JANAF tables[25] using the following relation,

$$\Delta_r G^\circ(T) = -RT \ln K_p(T). \qquad (12)$$

By definition of the standard state, the activity of the pure components or a compound in a pure phase is equal to unity since the departure from stoichiometric composition remains very small. For the equilibrium state in SiC with excess Si, $a_{Si} = 1$, a minimum carbon activity and the reverse for Si is obtained for a carbon-rich SiC. The isothermal variation in the activities in the SiC non-stoichiometric domain is displayed schematically in Fig. 5, by deliberately enlarging this non-stoichiometric domain. This kind of schematic representation provides a means of understanding how the partial pressures of the different vapour species vary in this non-stoichiometric composition domain connecting the two diphasic domains for which the exact gas composition is known, by starting for instance with equilibria of the form:

$$\text{Si (in SiC}_{(s,s)}) = \text{Si(g)} \quad K_p(T) = \frac{p_{Si}}{a_{Si}} \qquad (13)$$

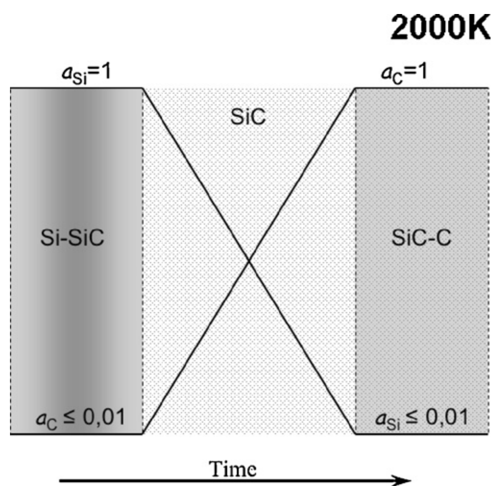

Fig. 5. Schematic isothermal evolution of the activities of Si and C components in the non-stoichiometric composition domain of SiC, displayed by enlarging intentionally this composition domain. The reference to time – in place of C composition – is used to show the composition evolution by vaporization losses.

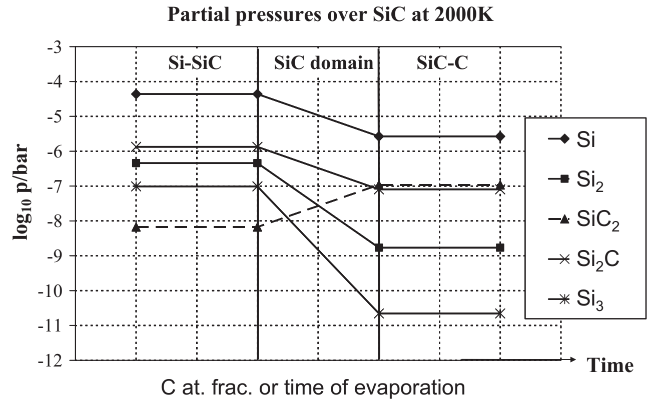

Fig. 6. Schematic isothermal evolution of the main partial pressures above SiC at 2000 K due to the change of condensed phase composition by material loss due to vaporization conditions. (The unknown non-stoichiometric composition domain of SiC has been intentionally enlarged.)

$$\text{Si (in SiC}_{(s,s)}) + \text{SiC(s, pure)} = \text{Si}_2\text{C(g)}$$

$$K_p(T) = \frac{p_{Si_2C}}{a_{Si}a_{SiC}} \qquad (14)$$

with $a_{SiC} = 1$. The partial pressures of the different gaseous molecules can now be calculated for each (unknown) composition included in the non-stoichiometric SiC composition domain using any activity (of Si or C) as a parameter. It is evident that the activities – which are monotonic functions of the composition – are located on the connecting lines of the two diphasic domains that bracket the SiC non-stoichiometric domain. As the thermodynamics of the SiC non-stoichiometric domain is not described, the activities have been schematically drawn as straight lines, but really and according to the nature of the existing point defects the connecting lines would be more or less S-shaped curves.

The modification in partial pressures results from the change in condensed phase composition caused by the material vaporization. Fig. 6 displays the above reasoning: partial pressure values are located necessarily between the two calculated extremes, *i.e.*, those of the two diphasics: they correspond approximately to the straight lines connecting the partial pressure values in the two-phase domains Si–SiC to SiC–C.

The non-stoichiometric composition of the SiC solid phase will change because of the evaporation flows. The silicon and carbon flows were first calculated in moles per second per unit area (1 m^2) as a function of temperature for the two limiting two-phase domains (diphasics). They are displayed in Fig. 7. Different cases can occur:

- For an Si–SiC diphasic mixture – SiC with Si impurities as precipitates – the C evaporated flow can come only from SiC, so this carbon flow can be considered to be equal to the SiC erosion. This kind of reasoning based only on C matter flow may appear incorrect because it seems that the SiC erosion is being underestimated as Si flow is known to be always greater than C flow and causes deposition of carbon in the form of graphite. In fact, for a two-phase Si–SiC mixture, graphite cannot be deposited as long as the two-phase compound is

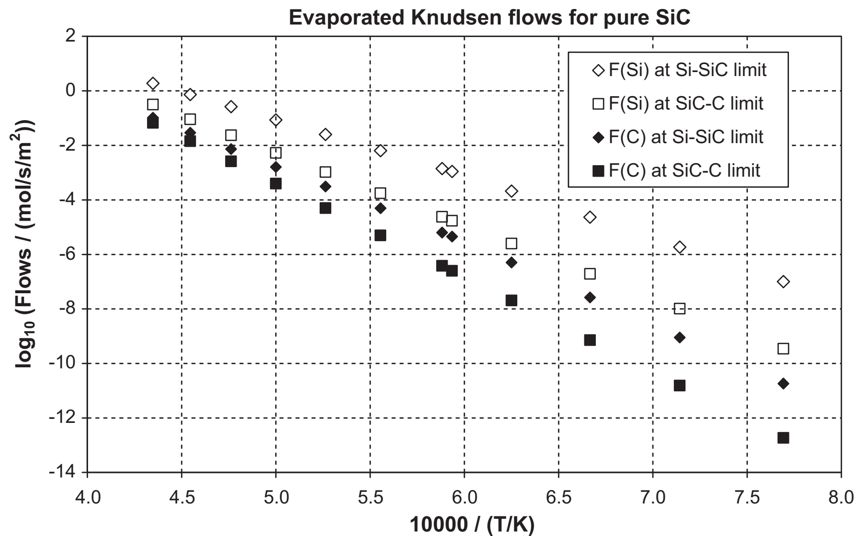

Fig. 7. The evaporated Si-flow and C-flow (or atomic erosion flows) from SiC (in moles per second per unit of surface) as a function of temperature for the SiC compound at its limits, Si–SiC and SiC–C, calculated from the equilibrium partial pressures.

being vaporized. So the escaping gaseous carbon – mainly in the form of $Si_2C(g)$ and $SiC_2(g)$ etc. – is the only cause of SiC erosion and the Si gaseous excess flow comes from the only free Si, rapidly causing further total loss of the initial excess of Si. Therefore,

$$F_{SiC}^{erosion} = F_{C}^{evap} \tag{15}$$

$$F_{Si}^{erosion} = F_{Si}^{evap} - F_{C}^{evap} \tag{16}$$

- For an SiC compound rich in Si – *i.e.*, at its SiC diphasic limit with Si that is at the disappearance of initial Si impurities – the SiC erosion will depend on the maximum flow among its components which is now the Si flow. The excess Si loss compared to C then causes the composition to tend towards SiC rich in C. At its SiC diphasic limit with Si, the erosion flow is equal to the Si evaporated flow and this situation pertains for the whole non-stoichiometric SiC domain since the Si loss – coming necessarily from the SiC compound – is always larger than the C loss:

$$F_{SiC}^{erosion} = F_{Si}^{evap} \tag{17}$$

- For an SiC compound that tend to be saturated with C (at the limit of the diphasic SiC–C), the total Si evaporated flow must be equal to the SiC erosion – *i.e.*, same features as above in the full non-stoichiometric composition range of SiC.

- For an SiC–C mixture – or SiC with C impurities or C precipitates as a result of previous excess loss of Si – the excess Si in the vapour phase can come only from the SiC and the erosion rate of SiC remains the same as for the above limit SiC–C applying relation (17). Thus, C accumulates at the surface of the SiC phase. This also means that any initial C impurity cannot be removed from a pure SiC compound by vaporization and the accumulation of C (or C growth) is,

$$F_{C}^{accumulation} = F_{Si}^{evap} - F_{C}^{evap} \tag{18}$$

3.4. Erosion of SiC compound grains by vaporization

Concerning the practical aspects of SiC transport and growth processes occurring during high-temperature sintering or recrystallization of SiC parts, the erosion of SiC was calculated as a layer thickness, *i.e.*, in micrometers per hour (μm/h) as displayed in Fig. 8 and Table 2 for the vaporization process under

Table 2
Decimal logarithm of SiC erosion rate ($\log_{10}$(erosion/μm/h) = $A/(T/K) + B$) and associated time to cross the stoichiometric SiC domain ($\log_{10}$(time/s) = $A/(T/K) + B$) for a defined layer thickness as an inverse function of temperature. $T = 1685$ K is the melting point of Si.

Coefficients	*A*		*B*	
Temperature domain	$T < 1685$ K	$T > 1685$ K	$T < 1685$ K	$T > 1685$ K
Si-rich SiC limit	−23,009.7	−20,330.7	15.35177	13.75509
C-rich SiC limit	−26,730.2	−26,794.4	15.75442	12.78299
Time (/s) to cross the SiC non-stoichiometric domain as defined in the text				
1 μm layer	23,039	20,680	−15.1202	−13.7083
10 μm layer	23,039	20,680	−14.1202	−12.7083

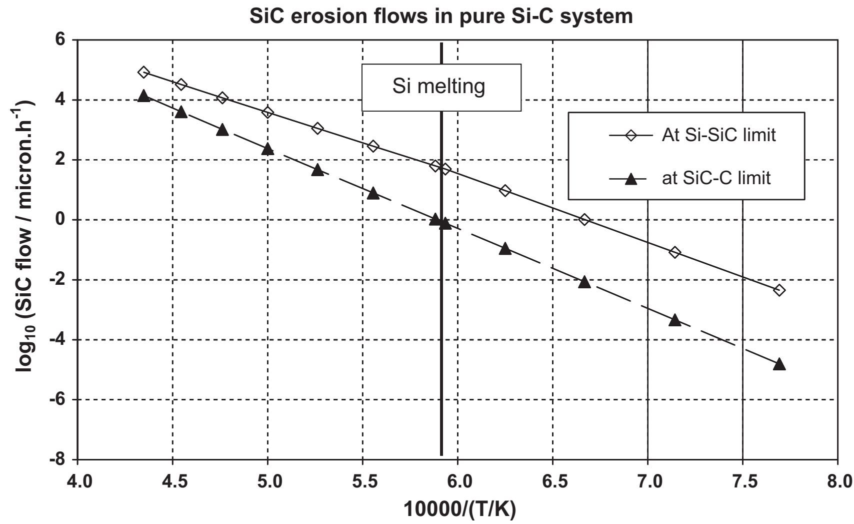

Fig. 8. The erosion rate of SiC calculated as a layer in μm/h as a function of the inverse of temperature for the two SiC non-stoichiometric compound limits calculated from the equilibrium partial pressures in a pure neutral gas.

vacuum (maximum erosion rate available at the surface, *i.e.*, Knudsen flow). The relation used is,

$$F_i^{\text{erosion}}(\mu\text{m h}^{-1}) = \frac{F_i^{\text{evap}}(\text{mol s}^{-1}\text{ m}^{-2})}{(d_i/M_i)\cdot 10^{-6}}\cdot 3600 \tag{19}$$

d being the density and *M* the molar mass for the corresponding solid *i* expressed in MKSA units. The product $(d/M)\cdot 10^{-6}$ is in fact the number of moles in a volume of 1 m^2 by 1 μm height. These total SiC erosion rates are calculated on the basis of the Si vaporization flows for the two SiC non-stoichiometric limits, *i.e.*, SiC rich with Si and SiC rich with C as explained above.

From the above explanations it is possible to calculate the time necessary for an Si-rich SiC compound (at the limit of the two-phase Si–SiC) to turn into SiC–C (other limit) by vaporization if the composition range of the non-stoichiometric domain of SiC is known. Two values for this non-stoichiometric composition range have been published[35,36] the first being about 1% and the later value ≤0.1%. This time is represented as a function of temperature considering arbitrarily a 0.1% change in non-stoichiometric composition as reported by Birnie and Kingery,[36] *i.e.*, $Si_{0.5}C_{0.5}$ turn into $Si_{0.499}C_{0.501}$. In this case, this means that for an arbitrarily chosen volume of SiC phase – the layer volume $V_L = (1\text{ m}^2\cdot 1\ \mu\text{m})$ – 0.1% of the SiC moles contained in this volume turn into C(s) by the loss of Si moles under equilibrium vaporization conditions: this corresponds to a volume equal to $v = V_L\cdot 10^{-3}$. Time necessary to cross the non-stoichiometric domain for a 1 μm is then,

$$t_{\text{cross}}(\text{s}) = \frac{((d_{\text{SiC}}/M_{\text{SiC}})\cdot 10^{-9})}{F_{\text{Si}}^{\text{evap}}}\quad (\text{mol m}^{-2}\text{ s}^{-1}) \tag{20}$$

The present relation operates for an isolated grain 1 μm diameter because there is no other source of silicon, but it is an

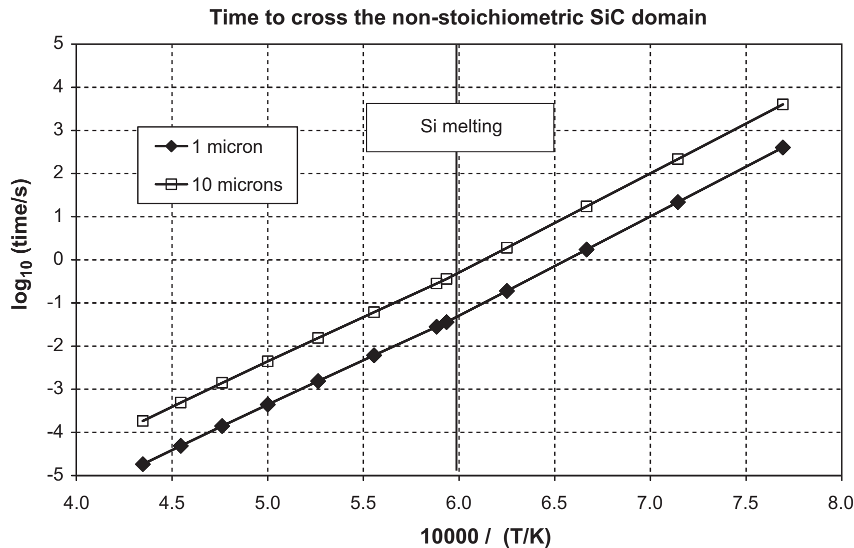

Fig. 9. Vaporization time necessary to turn a $Si_{0.5}C_{0.5}$ compound into a $Si_{0.499}C_{0.501}$ due to matter loss via (free) vaporization as a function of the inverse of temperature for a 1 and 10 μm thickness layer. The calculation was performed using the average Si flow between the two diphasics Si–SiC and SiC–C.

approximation for a real layer under equilibrium vaporization since the surface of the layer recedes with the evaporation flow of carbon and the layer thickness is regenerated by the SiC substrate material. The time to cross the non-stoichiometric domain for 1 μm layer becomes,

$$t_{\mathrm{cross}}(\mathrm{s}) = \frac{((d_{\mathrm{SiC}}/M_{\mathrm{SiC}})\cdot 10^{-9})}{(F_{\mathrm{Si}}^{\mathrm{evap}} - F_{\mathrm{C}}^{\mathrm{evap}})} \quad (\mathrm{mol\ m^{-2}\,s^{-1}}) \tag{21}$$

As the flow of carbon is always <1% of the silicon flow, there is practically no differences between the results according to relations (20) and (21). Fig. 9 (and Table 2) shows this "time to cross the non-stoichiometric domain" for a vaporizing powder of 1 and 10 μm SiC thickness (or ≈grain diameter). The calculations were performed with the average Si flow between Si-rich and C-rich SiC (assumption of a linear behaviour for pressures in the non-stoichiometric domain as mentioned above).

It is clear that the "time of existence" of a pure SiC powder grain of 1 or 10 μm size as an initial pure single-phase SiC placed under equilibrium vaporization conditions becomes very restricted with increase in temperature. For example at 1400 K a time of approximately 22 s is needed, while at 1600 K this time drops to about 0.2 s, at 1800 K to $3\cdot10^{-3}$ s and at 2000 K to only $4\cdot10^{-4}$ s in order to turn a 1 μm thick layer of Si-rich SiC into an SiC compound that starts to precipitate C at the surface. However, these calculations minimize the time because they are based on the available maximum mass loss flows under vacuum without no back condensation.

These calculations are based on the simple assumption that the vaporization phenomena are not limited by bulk diffusion of Si in SiC and by diffusion of the main vaporized species in a neutral gas flow. If the Si evaporation flow were to be limited by bulk diffusion, carbon would appear sooner at the surface, with the reverse effect if the limitation were to be a result of diffusion in neutral gas. Using XPS and AES Muehlhoff et al.[32] observed differently terminated faces of SiC crystals under high vacuum. Between 900 and 1300 K they found both initial Si-terminated and C-terminated faces covered with a carbon layer. Above 1300 K the massive graphitization of both surfaces is attributed by these authors to excess Si(g) vaporization from SiC surfaces, equivalent to the calculations described here. Note that with XPS and AES the observations are limited to just a few atomic layers while our calculations for 1 μm correspond to about 10,000 atomic layers and the above calculated time must be divided by $\approx10^4$ for comparison with their experiments. Note that for low temperatures, the bulk diffusion rate remains predominant compared to the evaporation rate (due to relative values of the activation enthalpies) and the carbon-rich surface structures can appear as predicted by our calculations without diffusion limitations.

4. Si–C–O ternary system

SiC, like other Si compounds, builds a SiO_2 protective layer under oxidative conditions, in air for example, but also under vacuum. SiC can therefore be considered to be always present as a ternary Si–C–O compound rather than pure SiC. Moreover,

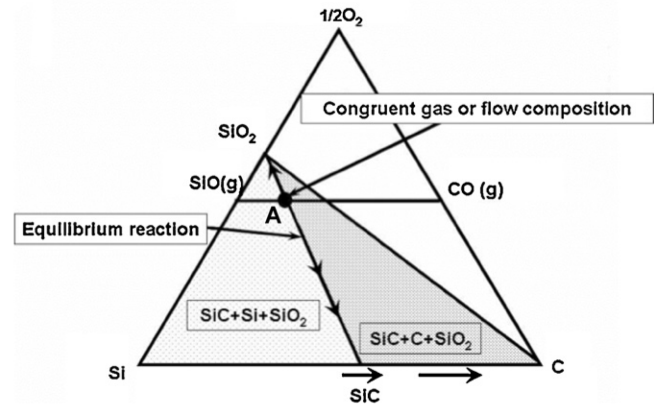

Fig. 10. Isothermal cross section of the ternary diagram of Si–O–C at least up to 1700 K. The arrows correspond to composition evolution due to vaporization.

because of its restricted non-stoichiometric domain and due to evaporation processes in manufacturing, SiC is relatively difficult to obtain in a pure SiC non-stoichiometric compound and it will be either rich in Si or in C, and always with the two components, a fact which means that equilibrium conditions were not reached in the last step of manufacturing by temperature decrease. The same features are true for the ternary compounds and, as a result, the vaporization behaviour of the so-called pseudo-binary compound SiO_2–iC and its mixtures with Si or C impurities has to be assessed to complete the study of SiC vaporization behaviour.

4.1. Vaporization in the Si–C–O ternary system

Fig. 10 presents a section of the Si–C–O condensed ternary system at $T = 1700$ K and 1 bar external applied pressure. The section of interest for the present investigation is the connecting line between SiC and SiO_2, which is also known as a pseudo-binary section.

Because Si- and C-rich compositions are being considered, the compositions near this line are also included. A band of compositions near this line must be examined, *i.e.*, the Si–SiC–SiO_2 and SiC–SiO_2–C three-phase domains (triphasic domains).

For the SiC–SiO_2 pseudobinary section - the two compounds being supposed as line compounds (rigourously stoichiometric compounds) –the main vaporization reaction, as already reported for instance by Jacobson and Opila[37] and Rocabois et al.[18] is:

$$\mathrm{SiC(s)} + 2\mathrm{SiO_2(s)} = 3\mathrm{SiO(g)} + \mathrm{CO(g)} \quad \text{with}$$

$$K_p(T) = \frac{p_{\mathrm{SiO}}^3 \cdot p_{\mathrm{CO}}}{a_{\mathrm{SiC}} \cdot a_{\mathrm{SiO_2}}^2}. \tag{22}$$

The variance for a closed system comprising initial mixture of n_1 fixed moles of SiC + n_2 fixed moles of SiO_2 as strictly stoichiometric compounds is:

$$v = c - r + 2 - \varphi = 1 \tag{23}$$

with the number of independent components $c = 3$ (3 components Si, C, O), r the number of constraints (1 relation (or constraint) to impose the composition on the line SiC–SiO_2) + 2

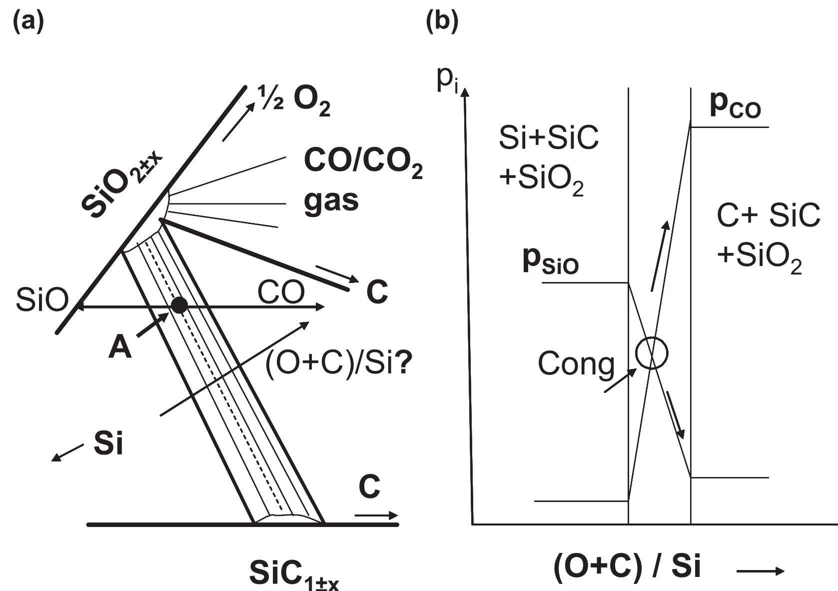

Fig. 11. (a) Schematic details of the isothermal equilibrium tie lines between the two "non-stoichiometric" compounds SiO_2 and SiC in the pseudobinary section SiC–SiO_2. (b) Going from the two triphasics Si–SiC–SiO_2 to SiC–SiO_2–C the partial pressures of the two main species SiO(g) and CO(g) crosses at a composition which is close to the congruent or azeotropic (quoted as "Cong") composition as discussed in the text.

external applied variables (T and p) − 3 phases (2 non-miscible solids + 1 gas). Fixing the temperature T the variance v becomes equal to 0. This means that the pressure – as we consider a gas phase – cannot be imposed externally but is imposed by the system, *i.e.*, p(total) = p(SiO) + p(CO). Under Ar – one more component – but with a fixed total pressure (1 bar for instance due to the presence of a permanent gas) the variance is the same. When fixing the temperature the final state of the system is also fixed: SiO(g) and CO(g) will mix in the Ar atmosphere with their equilibrium pressure (indirectly the volume is at that time fixed by the sum of the SiO(g) + CO(g) + Ar(g) partial pressures).

For an open SiC + SiO_2 system where the pressure of one gas – for instance CO(g) at a value included within the two triphasic domains Si–SiC–SiO_2 and SiC–SiO_2–C – can be imposed, the main equilibrium (22) will produce or decrease the SiC and/SiO_2 amounts, and the initial total composition moves. Varying the CO(g) pressure in the full available range compatible with the diphasic SiC–SiO_2 will show a minimum of the Gibbs energy of the only gas phase (solid phase is fixed) as calculated by Jacobson and Opila.[37] This minimum is necessarily the congruent (or azeotropic) state and the partial pressure ratio SiO/CO = 3/1 as proposed by Rocabois et al.[18] and corresponding to the Gibbs–Konovalov[38] rule. In the present case the gas composition corresponds to point A in Fig. 10.

Regarding the thermodynamics of the whole phase diagram, *i.e.*, the ternary Si–C–O system – it should be noted that the two $SiC_{1\pm y}$ and $SiO_{2\pm x}$ compounds have small but definitely non-stoichiometric domains, and tie lines characterize their equilibrium conditions, as sketched in Fig. 11a. Thus, with the initial compositions of the two compounds fixed and introducing a fixed mole number for each, the variance of a closed system is calculated as with the stoichiometric compounds but the constraint is now the line between the two non-stoichiometric compounds as shown in Fig. 12 (thick dashed line) and the main vaporization reaction at equilibrium will be,

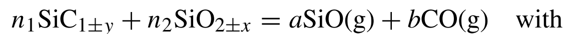

$$n_1 SiC_{1\pm y} + n_2 SiO_{2\pm x} = a SiO(g) + b CO(g) \quad \text{with}$$

$$K_p(T) = \frac{p_{SiO}^{a} \cdot p_{CO}^{b}}{a_{SiC}^{n_1} \cdot a_{SiO_2}^{n_2}}. \tag{24}$$

The equilibrium point is presented in Fig. 12 by a tie-line that cross the initial composition line (thick dashed line) at the initial composition ratio n_1/n_2. For an open system the initial composition of which can move when imposing for instance a CO(g) pressure, the equilibrium will correspond to a particular tie-line. Varying the CO(g) pressure one of these tie-line will correspond

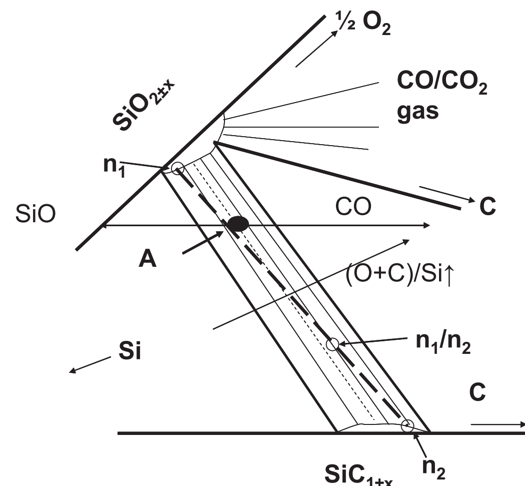

Fig. 12. Equilibrium conditions of a closed system obtained from the mixture of n_1 moles of $SiO_{2\pm x}$ and n_2 moles of $SiC_{1\pm y}$ non-stoichiometric compounds. The equilibrium conditions correspond to the tie-line crossing the initial amounts (thick dashed line n_1–n_2). The A composition is the congruent gas composition located on the congruent tie-line (thin dashed line).

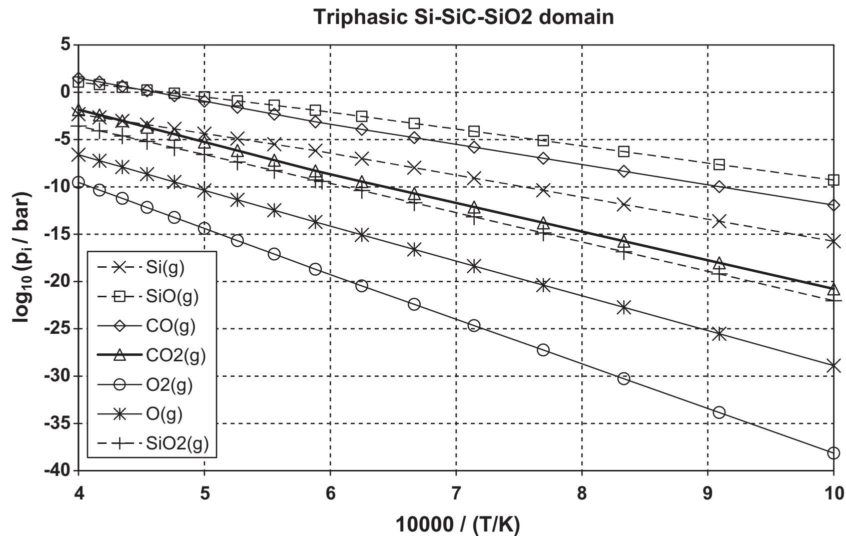

Fig. 13. Decimal logarithm of partial pressures in equilibrium with the three phase domain Si–SiC–SiO_2 as a function of the inverse of temperature. Note that above the melting point of Si at $T = 1685$ K the slope of the curves changes. Other gaseous species based on Si and C behaves according to the Si–SiC system (see Fig. 2 and Table 1).

to a minimum in the total pressure with the p(SiO)/p(CO) ratio equal to $a/b = 3/1$ (crossing the thin dashed line).

Thus, when the entire composition of the condensed phase moves from the Si–SiC–SiO_2 three-phase system to the SiC–SiO_2–C three-phase system crossing the pseudobinary section the partial pressures of SiO and CO vary as shown in Fig. 11b, at least for temperatures lower than 1900–2000 K and the total pressure produced by the system presents a minimum for compositions close to the crossing of partial pressures of these two species, as already explained by Rocabois et al.[18] and the gas composition at that time is located at point A in Figs. 10, 11 or 12. This minimum corresponds to a "partial" (because only composition ratios are fixed) azeotropic vaporization state for which the pseudobinary sample will loose a gas at the A composition located in the pseudobinary section meanwhile the remaining solid phase composition follows the "congruent" tie line that includes point A. Depending on the initial solid composition located between either A and SiC or A and SiO_2 (Fig. 10) the sample will loose preferentially either SiO_2 or SiC respectively. In the case of SiC samples with silica pollution, any heat treatment will vaporize first the initial (native or doped) SiO_2 content by vaporization.

First, in order to take into account the presence of Si or C impurities in the SiC green powders before any heat treatment, matter flows will be calculated from equilibrium partial pressures for every condensed mixture of SiC and SiO_2 compounds included in their near non-stoichiometric domains: Figs. 13 and 14 show the logarithmic plots of these partial pressures as an inverse function of temperature respectively for Si-rich and C-rich compositions, *i.e.*, Si–SiO_2–SiC and

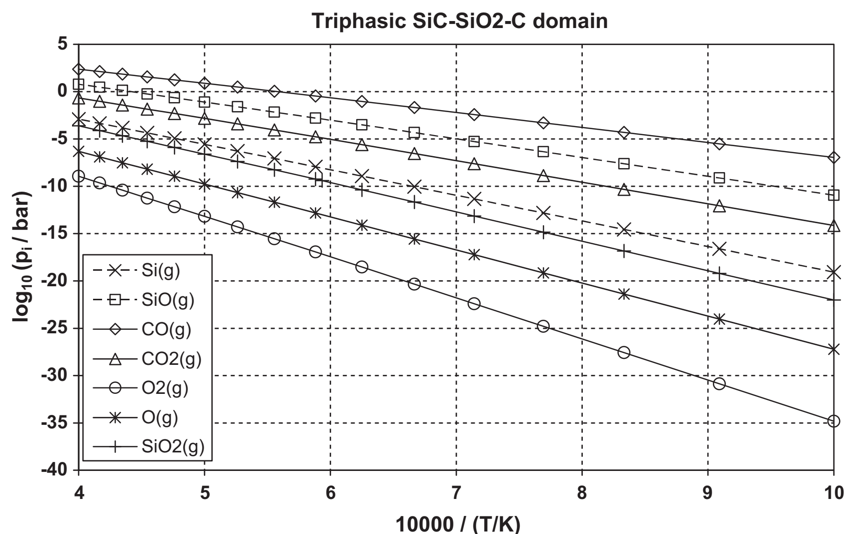

Fig. 14. Decimal logarithm of partial pressures in equilibrium with the three phase domain SiC–SiO_2–C as a function of the inverse of temperature. Other gaseous species based on Si and C behaves according to the SiC–C system (see Fig. 3 and Table 1).

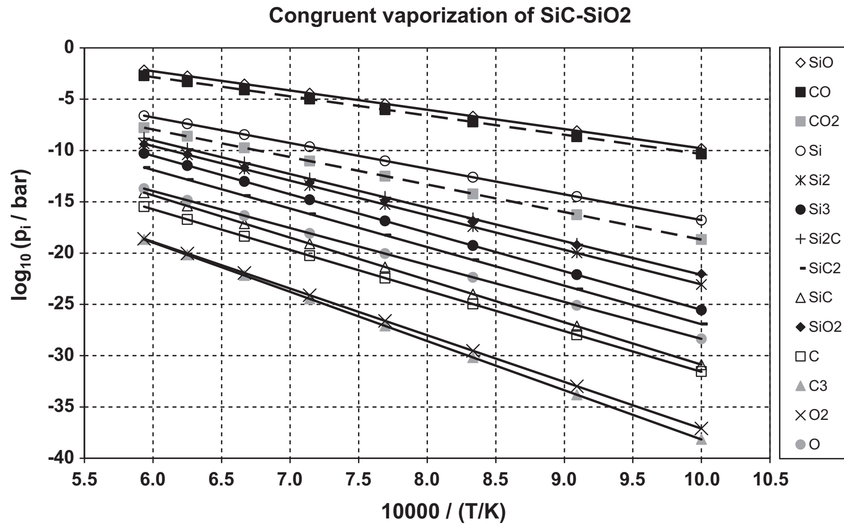

Fig. 15. Decimal logarithm of partial pressures over SiC–SiO$_2$ mixture for congruent vaporization (under vacuum) in the pseudo-binary section as a function of the inverse of temperature.

SiO$_2$–SiC–C three-phase domains respectively ($v = 0$ for fixed T, and the partial pressures are imposed by the set of condensed phases).

To calculate the partial pressures of SiO(g) for the Si-rich compounds mixtures reaction (25) was used:

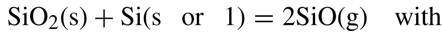

$SiO_2(s) + Si(s \quad or \quad 1) = 2SiO(g) \quad with$

$$K_p(T) = \frac{p^2_{SiO_2}}{a_{Si} \cdot a_{SiO_2}}. \tag{25}$$

Then, given that the value of $K_p(T)$ is known from the main vaporization reaction (22), the partial pressure of CO(g) is obtained. Other gases characteristic of Si-rich SiC have the same values as already calculated and described for the adjacent Si–SiC system in Section 3. For the C-rich compounds, the main reaction (26) is used,

$SiO_2(s) + 3C(s) = 2CO(g) + SiC(s) \quad with$

$$K_p(T) = \frac{p^2_{CO} \cdot a_{SiC}}{a^3_C \cdot a_{SiO_2}} \tag{26}$$

where the activities of solid or liquid phases are equal to 1.

Second, matter flows from pure SiC–SiO$_2$ pseudo-binary mixtures – *i.e.*, mixtures that have lost their Si or C impurities – will be calculated from partial pressures of the congruent vaporization of pure SiC + SiO$_2$ mixtures according to reaction (22) as presented in Fig. 15.

In a first attempt, the condition from the Gibbs–Konovalov theorem[38] was used, whereby for a fixed SiC/SiO$_2$ composition, the pressure will be an extremum for a system which has an "indifferent" (*i.e.* azeotropic or congruent (total or partial)) state. So for the congruent behaviour of the pseudo-binary SiC–SiO$_2$ system and taking into account only the main species SiO(g) and CO(g), the total pressure must be:

$$p_{tot} = p_{SiO} + p_{CO} \tag{27}$$

and using K_p from relation (22)

$$p_{tot} = p_{SiO} + \frac{K_p}{p^3_{SiO}} \tag{28}$$

and finally by derivation relative to SiO (gas composition in the SiO–CO coordinates),

$$\frac{dp_{tot}}{dp_{Sio}} = 1 - 3\frac{K_p}{p^4_{SiO}} \tag{29}$$

with an extremum for a zero value is obtained for,

$$p_{SiO} = 3p_{CO} \tag{30}$$

and so,

$$p^{Congruent}_{SiO} = (3K_p)^{1/4}. \tag{31}$$

When material vaporization under Knudsen conditions is considered, *i.e.*, absolute (pure) vacuum, the flow of different species must be addressed rather than their partial pressures. This means that the partial pressure ratio at the congruent state will be different as explained already for the Si–C system. For congruent flow conditions, consideration must be given to:

$$F_{SiO} = 3F_{CO} \tag{32}$$

and using the Knudsen relation for flows,

$$p_{SiO} = 3\sqrt{\frac{M_{SiO}}{M_{CO}}}p_{CO} = 3.76p_{CO}. \tag{33}$$

This relation shows that, in the case of vaporization under vacuum, the pressure ratio of SiO and CO is higher (=3.76) than for the pressures under neutral gas atmosphere or closed vessel (=3) as already discussed by Rocabois et al.[18] in the vaporization of based silicon compounds. The SiO congruent pressure is then,

$$p^{Congruent}_{SiO} = \left[3\sqrt{\frac{M_{SiO}}{M_{CO}}}K_p\right]^{1/4} = (3.76K_p)^{1/4} \tag{34}$$

Table 3
A and *B* coefficients for the decimal logarithmic plot of partial pressures according to $\log_{10}(p/\text{bar}) = A/(T/\text{K}) + B$. For the Si-rich compositions above the Si melting temperature of 1685 K, the slope will change and a similar effect will be found above the silica melting point. Note that for the SiC(g) and SiO2(g) species the quoted values are in principle similar due to equilibrium with the pure (same stoichiometry) compounds.

Coefficients	*A*		*B*	
$Si–SiC–SiO_2$ mixtures	*T* < 1685 K[a]	*T* > 1696 K	*T* < 1685 K	*T* > 1696 K
SiO	−17,957	−15,948	8.6842	7.4857
CO	−21,254	−24,839	9.3538	11.481
CO_2	−30,202	−34,778	9.4289	12.143
SiO_2	−31,034	−30,229	9.0097	8.5275
O	−36,855	−37,846	7.9715	8.5585
O_2	−47,154	−49,135	9.0120	10.186
Other species as in Table 1 for Si–SiC				

Coefficients	*A*	*B*
$SiC–SiO_2$ congruent	*T* < 1950 K	T < 1950 K
SiO	−18,815	9.0253
CO	−18,748	8.4017
CO_2	−26,862	8.1647
Si	−24,998	8.2200
Si_2	−33,736	10.685
Si_3	−37,539	12.010
Si_2C	−32,763	10.648
SiC_2	−37,550	10.628
SiC	−41,249	10.377
SiO_2	−31,058	9.0364
C	−39,551	7.9951
C_3	−47,963	9.8022
O	−36,025	7.6616
O_2	−45,494	8.3922

Coefficients	*A*		*B*	
$SiC–C–SiO_2$ mixtures	*T* < 1685 K[a]	*T* > 1696 K	*T* < 1685 K	*T* > 1696 K
SiO	19,834	18,938	8.9028	8.3670
CO	15,678	15,197	8.7574	8.4731
CO_2	22,776	21,809	8.6436	8.0717
SiO_2	31,062	29,893	9.0396	8.3454
O	35,005	34,520	7.7827	7.4951
O_2	43,454	42,483	8.6343	8.0591
Other species as in Table 1 for SiC–C				

[a] This temperature corresponds to the silicon melting temperature, while the other corresponds to the silica melting point (based on JANAF tables[25]).

In the present work the congruent vaporization (under vacuum) has been calculated by two different ways, either using the above Gibbs–Konovalow[38] theorem applied to the only SiO and CO main species as above, or solving with the complete set of species in order to check the influence of minor gaseous species on the gas phase composition at the congruent state.

In the first way, with $SiC–SiO_2$ mixtures, the partial pressures of the minor species are deduced from the SiO and CO above calculated congruent pressures from relations (27)–(34) and using different equilibria such as, $SiO_2 + Si(g) = 2SiO(g)$ with

$$SiO_2 + Si(g) = 2SiO(g) \quad \text{with} \quad K_p(T) = \frac{p_{SiO}^2}{a_{SiO_2} \cdot p_{Si}} \quad (35)$$

$$2Si(g) = Si_2(g) \quad \text{with} \quad K_p(T) = \frac{p_{Si_2}}{p_{Si}^2} \quad (36)$$

$$Si(g) + SiC(s) = Si_2C(g) \quad \text{with} \quad K_p(T) = \frac{p_{Si_2C}}{a_{SiC} \cdot p_{Si}^2} \quad (37)$$

$3SiC(s) + CO(g) = 2SiC_2(g) = SiO(g)$ with

$$K_p(T) = \frac{p_{SiC_2}^2 \cdot p_{SiO}}{a_{SiC}^3 \cdot p_{CO}} \quad (38)$$

To obtain the partial pressure of CO_2 the equilibrium (39) was considered for the congruent condition and Si(g) pressures and equation (40) for the congruent condition and the C activity:

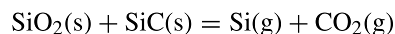

$SiO_2(s) + SiC(s) = Si(g) + CO_2(g)$

$$K_p(T) = \frac{p_{Si} \cdot p_{CO_2}}{a_{SiC} \cdot a_{SiO_2}} \quad (39)$$

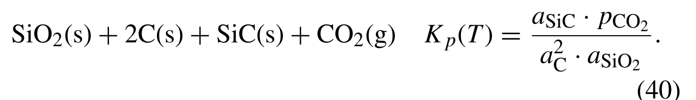

$$SiO_2(s) + 2C(s) + SiC(s) + CO_2(g) \quad K_p(T) = \frac{a_{SiC} \cdot p_{CO_2}}{a_C^2 \cdot a_{SiO_2}}. \quad (40)$$

The second way, an alternative and more accurate method, involves considering the calculation of the vaporization flows

(Knudsen flows) of all species and the congruent relation for the gas composition is then deduced from the flow composition imposed in the pseudo-binary system $SiC–SiO_2$ (composition on the line $SiC–SiO_2$). The congruent flow relations, as already proposed for pseudobinary sections by Banon et al.,[39] or Malheiros et al.,[40] are derived from the following reasoning: (i) the part of the Si flow corresponding to SiC vaporization is equal to the C vaporization and (ii) the part of the Si flow corresponding to SiO_2 vaporization is equal to half the oxygen flow,

$$F'_{Si} = F_C \quad \text{and} \quad F''_{Si} = \frac{1}{2}F_O \tag{41}$$

and the total Si flow is,

$$F_{Si}^{Total} = F_C + \frac{1}{2}F_O \tag{42}$$

and the congruent (azeotropic) state is calculated checking relation (42) when the activity of Si is varied within the non-stoichiometric range of SiC, *i.e.*, from the SiC–C limit to the Si–SiC ($a(Si) = 1$) limit.

The two methods for calculating the congruent partial pressures give very similar results up to the 1900–2000 K range. At that temperature, the $SiC–SiO_2$ system cannot vaporize congruently since the CO pressure becomes higher than the SiO pressure while the silicon activity reaches the value 1, *i.e.*, the $Si–SiC–SiO_2$ phase limit, and the liquid silicon phase appears. This is how silicon production is managed in arc-melting furnaces.

Table 3 lists the coefficients *A* and *B* for the decimal logarithmic plots of the partial pressures as an inverse function of temperature for the different composition domains analysed above.

4.2. Change in composition due to vaporization losses

The main question in calculating erosion by vaporization of SiC-based compound materials which contain additives such as Si, C or SiO_2, is to identify the losses that can be attributed to the erosion of SiC, SiO_2 or impurities.

For the only pure pseudo-binary system $SiC–SiO_2$ that vaporizes under congruent conditions (absolutely neutral atmospheric conditions or pure absolute vacuum), the Si atomic vaporization flow represents the erosion of SiC and of SiO_2 at the same time according to reaction (22). The origin of the C flow can only be the SiC compound. So the part of Si flow resulting from SiC erosion must be equal to the C evaporated flow measured in moles per second for a 1 m^2 evaporating surface. The remaining excess Si flow is thus attributed to SiO_2 erosion. Thus, as an example, erosion flows $F^{erosion}(mol\,s^{-1}\,m^{-2})$ are evaluated from the total atomic vaporization flows $F^{evap}(mol\,s^{-1}\,m^{-2})$ of C and Si according to the following relations,

$$F_{Si}^{evap} = F_{SiC}^{erosion} + F_{SiO_2}^{erosion} \tag{43}$$

$$F_C^{evap} = F_{SiC}^{erosion} = F_{Si}^{from\ SiC} \tag{44}$$

$$F_{SiO_2}^{erosion} = F_{Si}^{evap} - F_{SiC}^{erosion} = F_{Si}^{evap} - F_C^{evap} = \frac{1}{2}F_O^{evap} \tag{45}$$

For a Si-rich $SiC–SiO_2$ mixture (the $Si–SiC–SiO_2$ three-phase system) the different flows are more difficult to identify because the source of the Si evaporated flow can be SiO_2, SiC and Si in excess. However, the source of C flow can only be SiC, so the number of moles of vaporized C is equal to the erosion of SiC and to the number of Si moles resulting only from SiC. The erosion of SiO_2 must also be equal to half of the oxygen atomic flow which is also equal to the number of moles of Si from SiO_2. Then, the remaining Si flow is due to erosion of excess Si and so,

$$F_{SiC}^{erosion} = F_C^{evap} \tag{46}$$

$$F_{SiO_2}^{erosion} = \frac{1}{2}F_O^{evap} \tag{47}$$

$$F_{Si}^{erosion} = F_{Si}^{evap} - F_C^{evap} - \frac{1}{2}F_O^{evap} \tag{48}$$

Considering a condensed $SiC–SiO_2$ mixture rich in carbon, *i.e.*, the $SiO_2–SiC–C$ three-phase compound, SiC cannot be considered to be the only source of C flow. Furthermore, considering the reaction

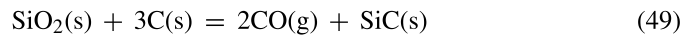

$$SiO_2(s) + 3C(s) = 2CO(g) + SiC(s) \tag{49}$$

for calculating the CO partial pressure of C-rich mixtures, it is found that in this case SiC is not eroded at all, but SiC is created from SiO_2 and free carbon. Like the Si-rich compound discussed previously, the erosion of SiO_2 is calculated as half of the oxygen atomic flow, *i.e.*, the relation (47). It follows that the same quantity of the total atomic evaporated flow of Si can be attributed to the effect of SiO_2 erosion and the remaining Si flow is related to SiC – erosion when >0 or growth when <0,

$$F_{SiC}^{erosion}\ (\text{if} > 0) \quad \text{or} \quad F_{SiC}^{growth}\ (\text{if} < 0) = F_{Si}^{evap} - \frac{1}{2}F_O^{evap} \tag{50}$$

Indeed, for this triphasic, the oxygen flow is coming from CO(g) and SiO(g) the partial pressures of which are far above the silicon gaseous species, and relation (50) gives the real growth of SiC detrimental to silica according to relation (49). The C atomic vaporization flow is equal to the erosion of carbon in excess of the growth, and is directly related to the CO(g) departure (remind that the pressure of CO(g) is the highest in this triphasic).

The C atomic vaporization flow is equal to the erosion of carbon in excess and

$$F_C^{erosion} = F_C^{evap} + \left|F_{SiC}^{growth}\right| = F_C^{evap} - \left|F_{Si}^{evap} - \frac{1}{2}F_O^{evap}\right|. \tag{51}$$

Thus, in the case of C-rich mixtures, no SiC erosion can be observed as long as SiO_2 and C are co-existing since the growth of SiC is operating detrimental to SiO_2 reacting with C according to reaction (49). An excess of C is eroded via the vaporization of the CO(g) species the pressure of which remain the highest one. Indeed SiC is created in this way by the carbothermal reduction of silica as it is the case during the first step of Si extractive metallurgy with an important loss of carbon in the gas phase.

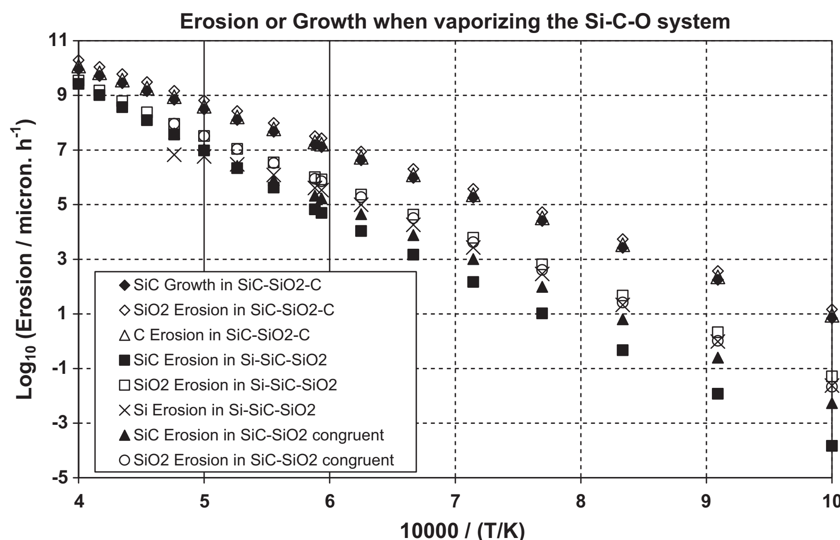

Fig. 16. Decimal logarithm of erosion or growth flows of SiC, SiO_2, Si and C during vaporization for the pure and congruent pseudobinary system SiC–SiO_2 and for the Si rich and the C rich SiC–SiO_2 triphasic mixtures in micron of eroded material per hour as a function of the inverse of temperature. Note that for the SiC–SiO_2–C system there is no erosion of SiC but growth.

Fig. 16 displays the different erosion (or growth when applicable) flows due to vaporization as described above. In order to facilitate their understanding, they are displayed as decimal logarithms as an inverse function of temperature. This figure shows that for the gas congruent compositions of the SiC–SiO_2 pseudo-binary compound, SiC like SiO_2 will be eroded continuously and uniformly as temperature increases with a slight change at the silica melting point. Indeed, the ratio of eliminated SiC and SiO_2 remains constant (main reaction (22)) by increasing amount of eroded material up to the end of the congruent vaporization (≈1950 K).

For Si-rich SiC–SiO_2 mixtures, excess Si will be eroded until about 1950 K due mainly to the SiO(g) pressure which is by far the main gaseous species. Above 2000 K the excess Si will not be eroded at all because, above this temperature, the SiC–SiO_2 pseudo-binary compound will no longer vaporize congruently and Si–SiC–SiO_2 three-phase mixtures are stable with Si (liquid) production: this is how silicon is produced in arc-melting furnaces. At the same time SiC erosion, which was initially lower than Si and SiO_2 erosion, increases until it is close to SiO_2 erosion above 2100 K.

For the C-rich SiC–SiO_2 mixtures, a constant ratio of erosion of C and SiO_2 is observed with a slightly higher SiO_2 erosion flow and SiC growth detrimental to C. This behaviour is due to the main chemical reaction considered in this section, but also during the experiments, and for the manufacturing process of SiC, SiC crystal growth is generally observed on carbon surfaces such as linings or furnace kilns made with graphite.

The behaviour described here and the calculated erosion rates show that impurities, such as Si or C in excess in initial SiC powders, are eliminated initially by primary vaporization–or SiC growth -from the components reacting with SiC or silica as already shown experimentally by S. Baud et al.[40] using mass spectrometry and finally a pure SiC–SiO_2 congruent mixture will be vaporized after a short while.

Unlike the SiC binary compound, calculation of the "time to cross the non-stoichiometric domain" of SiC in contact with SiO_2 would not be significant. This is explained by the fact that, due to congruent vaporization in the pseudobinary system, as long as SiO_2 is available, no change in SiC non-stoichiometric composition can take place during SiO_2 depletion due to a fixed tie-line during congruent vaporization. Once all SiO_2 is eliminated by vaporization, the first SiC residual crystals obtained are within the non-stoichiometric composition domain of the SiC compound corresponding to the congruent tie-line. Then, subsequently, the pure SiC compound residue behaves as described in the binary Si–C system, with further C(s) surface accumulation due to excess Si losses by vaporization.

The very high values of erosion rates at 2500 K – more than 1 m per hour – are related to the high pressures of SiO(g) and CO(g). These values cannot be reached in normal furnaces because certain limitations will occur due to the flow regime of the escaping gases and limitations of the applied pressure (close to 1 bar). Even so, at the beginning of the intermediate temperatures during the first step of the heat treatment, the quite high values of erosion rates explain the rapid distillation of any Si or silica impurities as well as the consumption of C impurities into SiC. During the next step, the congruent vaporization of SiC–SiO_2 mixtures, and due to the minimum total pressure, the erosion rates of SiC are rather low compared to the one close to the limit with carbon.

Table 4 lists the coefficients A and B for the decimal logarithmic plots of the erosion (or growth) rates as an inverse function of temperature for the different composition domains analysed above.

5. SiC re-deposition

In the previous section, the evaporated Si and C atomic flows from SiC were calculated and general erosion rates were

Table 4
Coefficients A and B for the decimal logarithm of erosion (or growth) rates by vaporization in the congruent SiC–SiO_2 pseudo-binary system and in the Si-rich and C-rich three-phase domains as an inverse function of temperature, $\log_{10}(\text{erosion}/\mu\text{m/h}) = A/(T/\text{K}) + B$.

Coefficients for the component or compound	A		B	
Congruent SiC–SiO_2[a]	1000–1685 K	1685–1950 K	1000–1685 K	1685–1950 K
SiO_2	−18,514	−17,616	16.846	16.307
SiC	−18,471	−17,617	16.198	15.688
SiC–SiO_2–Si (rich)[a]	1000–1685 K	1685–1950 K	1000–1685 K	1685–1950 K
SiO_2	−17,738	−18,551	16.454	16.861
SiC	−20,978	−24,405	17.149	19.181
Si	−17,612	−13,310	16.001	13.450
SiC–SiO_2–C (rich)	1000–1685 K	1685–2500 K	1000–1685 K	1685–2500 K
SiO_2	−15,411	−14,798	16.577	16.212
SiC growth	−15,404	−14,730	16.253	15.851
C	−15,406	−14,752	16.364	15.974

[a] Note that above 1950 K the pseudobinary does not vaporize congruently but produces liquid silicon.

obtained for any vaporization experiment. No attention was paid to the fact that some of these flows when transported in large parts through pores or holes can recombine on the surface of any other solid SiC crystal in the manufacturing furnaces. Indeed, due to mass loss by vaporization in non-closed containers as well as to reactions with the walls materials – since silicon and SiO(g) are very reactive gases and no inert containers are known – there exists always some chemical gradients due to transport by the gas phase from the inner volume to the outer surface of the manufacturing parts. Along this transport process the distillation of silica enhances at least an oxygen potential gradient across the parts. So, the vapours can condense and/or react either to form new SiC crystals or to grow new layers under the influence of any local chemical potential gradients (temperature is supposed homogeneous). This is for instance the case in the Lely growth refinement process for pure SiC growth crystals of different polytypes. The present part deals with the available flows for local SiC growth considering at first that the vaporization and condensation phenomena are at equilibrium and in an apparent quasi-homogeneous SiC material. Indeed, the real situation could be calculated only when the local composition (including pressures) gradients were known as it is usually the case in deposition processes for which the temperature gradients are fixed.

5.1. Pure SiC compound

The maximum SiC precipitation as a non-stoichiometric compound can come only from the reaction of silicon with carbon from the gaseous phase, *i.e.*, by vapour transport. It is equal to the only carbon flow resulting from gaseous species containing C, such as Si_2C, SiC_2, SiC, C, C_3, *etc.* since silicon is in excess and will be lost. Fig. 17 displays the available SiC

deposition rates from the C flows within the two SiC non-stoichiometric limits, *i.e.*, considering the whole existence domain of the SiC compound. In this figure, the SiC erosion flows for the same two-phase limits as calculated in part 3 are also displayed. Thus, for pure SiC the difference between erosion

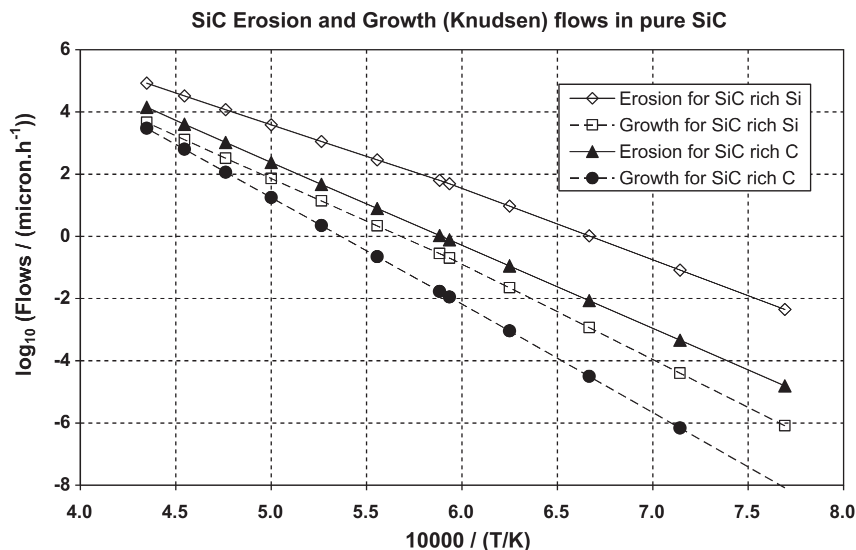

Fig. 17. Decimal logarithms of SiC available deposition rates from a SiC at its stoichiometric SiC rich Si and rich C and comparison with SiC erosion rates. All values are in μm of SiC per hour.

and deposition rates is always in favour of erosion regardless of the SiC near-stoichiometric composition. This feature is the consequence of the excess of Si in the vapour phase that erodes SiC more than C regardless of the near-stoichiometric composition of the solid.

5.2. *SiC–SiO_2 pseudo-binary mixtures*

For pure pseudo-binary mixtures, several mechanisms can occur simultaneously when including all the pure Si_xC_y gaseous molecules as discussed in the preceding section for pure SiC and adding the oxygenated species such SiO(g) and CO(g) that are produced by the main congruent vaporization (22). Two general growth mechanisms can occur:

- First, assuming that the gaseous species containing oxygen, CO(g) and SiO(g), can recombine to form solid SiC according to the reverse of the main congruent vaporization reaction as already postulated by Kreigesman et al.[41,42]

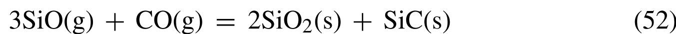

$$3SiO(g) + CO(g) = 2SiO_2(s) + SiC(s) \quad (52)$$

one mole of pure SiC can grow only if the SiO_2 and SiC grains are separated and if an equivalent growth of two moles of pure SiO_2 occurs. However, reaction (52) cannot occur simultaneously for two different and separate surfaces without postulating a certain specific energy associated with special sites and selective growth. Reaction (52) is probably produced on the same surface at the same time, and consequently "black glasses" are produced as observed for deposits in furnaces. Black glasses could therefore produce links between the SiC and SiO_2 grains or between two SiC grains (covered at least partly with a SiO_2 layer).

- Second, assuming that reaction (52) does not occur at the SiC surface and that pure SiC grains exist in the mixture (with a bare SiC surface), the same Si_xC_y gaseous species as for pure SiC can condense and lead to the growth of SiC grains. In this case SiC will grow with a near-stoichiometric SiC composition corresponding to that at the congruent interface SiC/SiO_2, *i.e.*, for the silicon activity (or oxygen activity) corresponding to this interface (along the congruent tie-line as discussed above), this silicon activity being between the two diphasic ones.

Furthermore, due to the known Si(g) species in excess in the only Si–C gaseous phase and to the presence of SiO(g) and CO(g) in the gas phase, other different reactions can produce SiC(s) precipitation, the main one being,

$$2Si(g) + CO(g) = SiC(s) + SiO(g) \quad (53)$$

and as a result half of the available excess Si-flow, which is not associated with carbon or oxygen in the gaseous phase, could be consumed for SiC deposition through an excess of CO(g) pressure at the SiC surface. Indeed, due to reactions with the kiln materials, excess CO(g) may become sufficient (but nonetheless small compared to the main Si(g) pressure) to act as a background component of the carrier or furnace gas. The SiC from this precipitation reaction added to SiC from carbon gaseous flow alone, leads to the maximum possible precipitation/condensation rate of SiC. Note that this possibility is dependent on any real counter-effect due to reaction (52), *i.e.*, to return to the real equilibrium conditions.

Fig. 18 displays the possible SiC minimum and maximum vapour phase deposition rates of any SiC–SiO_2 pseudo-binary composition mixture – some with excess Si, some with excess C – and compares these deposition rates with the erosion already calculated in the different three-phase systems. Note that the vapour phase deposition rates are the same as for the pure SiC compound (Fig. 17) at its non-stoichiometric limits since the same gaseous species that transport SiC have the same partial pressures. The available minimum or maximum SiC vapour phase deposition rates are much lower than the erosion rates for

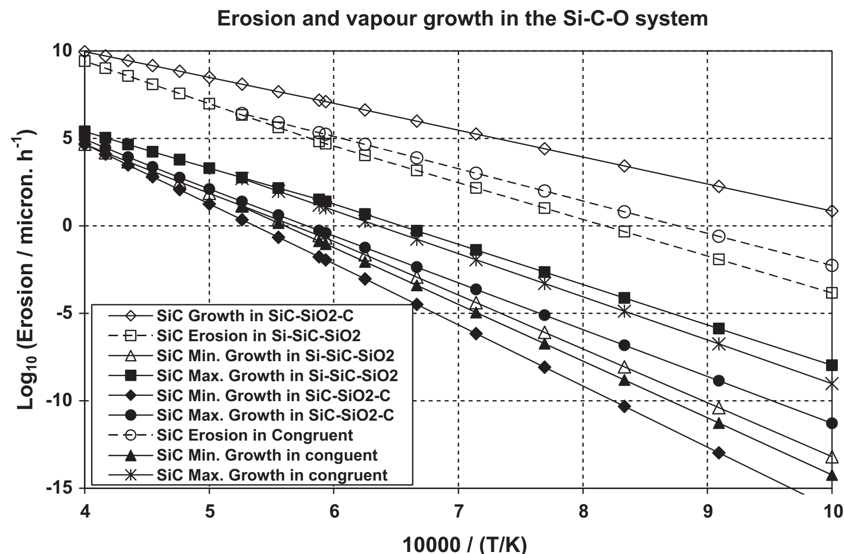

Fig. 18. Decimal logarithm of SiC vapour phase deposition rates from SiC–SiO_2 enriched with Si or with C. The erosion of SiC from the triphasic Si–SiC–SiO_2 as well as from the congruent SiC–SiO_2 and the growth of SiC from the triphasic SiC–C–SiO_2 are displayed for comparison. All values are in μm of SiC per hour.

an Si-rich SiC–SiO_2 mixture as well as for congruent pseudo-binary mixtures. For C-rich SiC–SiO_2 mixtures, the SiC growth from the reduction of SiO_2 by C is much higher than the available growth by the vapour phase of the SiC at its C-rich limit. This means that as soon as the excess C is consumed, the SiC growth is stopped while the SiC–SiO_2 mixtures become congruent and SiC erosion (at the pseudo-binary congruent vaporization) will start.

The main result is that during the heating phases in a furnace where any SiC + SiO_2 pseudo-binary mixture coexists with Si or C impurities or both, the Si impurity will be evaporated quickly while the C will produce SiC detrimental to silica. Once these impurities have been completely depleted, for the resulting SiC–SiO_2 pure pseudo-binary mixtures, SiC erosion becomes so great that no deposition of pure SiC can occur during this step before the complete disappearance of silica.

6. Summary and conclusions

The vaporization behaviour of Si–C binary and Si–O–C ternary systems is first described around compositions corresponding either to pure SiC or to mixtures of pure SiC + SiO_2 containing Si and C impurities and the various erosion flows (obtained by vaporization), *i.e.*, SiC, SiO_2, Si and C flows were evaluated. In a second step the possibilities of growth by vapour phase transport and condensation in parts under processing were also evaluated.

It was found that, for a pure Si–C binary system with increasing temperature, vaporization conditions always involve a loss of excess Si compared to carbon regardless of the SiC compound composition in its non-stoichiometric domain from silicon-rich to carbon-rich limits. It follows that any SiC material at high temperature under neutral vaporization conditions preferentially looses its Si impurities (if existing initially) and then turns rapidly into carbon-rich SiC composition, after which carbon precipitates at the surface at a rate equal to rate of loss of excess Si and finally SiC tends to become pure carbon or graphite by re-crystallization. Evaluation of vaporization rates on a thermodynamic basis, compared to reasonable estimates of the composition range of the non-stoichiometric domain of the SiC compound, shows that the precipitation of C becomes very high and rapid with increase in temperature as soon as 2100 K is reached (more than 100 μm/h). In any manufacturing process, these calculated times for this process show that it is impossible to prevent carbon precipitation when applying any external physical parameter, such as the total pressure applied to the system, pure neutral gas use or working in a strictly closed vessel. This is also the case when kiln structures are not inert.

The Si–O–C ternary system – around the SiC–SiO_2 pseudo-binary section – behaves differently due to the formation of SiO(g) and CO(g) gaseous species that are by far the main species. In this case the precipitation of carbon is not possible due to CO(g) formation. Partial pressures of oxygen-free species (Si, Si_2, Si_3, Si_2C, SiC_2, etc.) behave in the same way as for the Si–C binary system as long as no solid solutions are known between the different compounds and three-phase equilibria are established as in the Si–SiC–SiO_2 and SiC–SiO_2–C systems. The pure SiC–SiO_2 pseudobinary system vaporizes congruently and produces the two main gaseous species SiO(g) and CO(g): the interface potentials between the SiC and SiO_2 crystals then become fixed. It was shown that the partial pressures of the gaseous species are different for the Knudsen flow conditions (vacuum) and for flows under inert carrier gas atmosphere because in the first case flow compositions have to be taken into account and in the second case allowance must be made for the mole fractions in the gaseous phase to impose congruent conditions. In this study, the Knudsen flow conditions – corresponding to vacuum conditions and maximum surface flow rates – were used for most of the calculations in order to help understand the Knudsen cell mass spectrometric experimental results.

By making equilibrium assumptions for these flows of different components, Si, C, O, the origin of the erosion flows (by vaporization) for SiC, SiO_2, and the Si and C impurities can be calculated and distinguished. Given that the original SiC and SiO_2 powder mixtures are very often enriched with Si or C impurities, these calculated flow values show the quasi-immediate possibilities of purification in the early stage of heat treatment of green SiC parts. Then the parts vaporize congruently in the pseudobinary section. Moreover, the departure of oxygen (that is silica) is calculated and the compositional variation in the system at that time would be towards pure SiC (within its non-stoichiometric domain limits) as a stage before going to SiC–C system, *i.e.*, carbon precipitation at the surface of SiC grains soon after the loss of silica.

The possibilities of condensation and growth associated with the vaporization of the pure SiC–SiO_2 pseudobinary system showed that vapour phase growth processes can lead either to mixtures, usually called "black glasses", or occasionally to pure SiC if the surface of the SiC grains remains free from silica and if growth is associated only with the Si–C gaseous species (as in the pure Si–C system) that can be enhanced by some local CO(g) excess reacting with the available excess Si flow. Finally, in any case the use of silica additives cannot be considered as a direct growth agent.

Acknowledgments

The authors would like to thank the St-Gobain CREE research centre at Cavaillon (France) for sponsoring the present study.

References

1. Olesinski RW, Abbaschian GJ. The (C–Si) system. *Bull Alloys Phase Diag* 1984;**5**:527–8.
2. Dolloff RT. Research study to determine the phase equilibrium relations of selected metal carbides at high temperature. *WADD Tech Rep* 1960:60–143.
3. Kleykamp H, Schumacher G. The constitution of the silicon-carbon system. *Ber Bunsen-Ges Phys Chem* 1993;**97**:799–805.
4. Durand F, Duby JC. Carbon solubility in solid and liquid silicon. *J Phase Equilib* 1999;**20**:61–3.
5. Gröbner J, Lukas HL, Aldinger F. Thermodynamic calculation of the ternary system Al–Si–C. *Calphad* 1996;**20**:247–54.
6. SGTE. Thermodynamic properties of inorganic materials compiled by SGTE. In: Martienssen W, editor. *Landolt-Börnstein – numerical data*

and functional relationships in science and technology. Berlin, Heidelberg: Springer-Verlag; 2004. p. 140–2.

7. Kaufman L. Coupled phase diagrams and thermochemical data for transition metal binary systems IV. *Calphad* 1979;**3**:45–76.
8. Scace RI, Slack GA. Solubility of carbon in silicon and germanium. *J Chem Phys* 1959;**30**:1551–5.
9. Chatillon C. *Contribution à l'étude par spectrometry de masse des phases métalliques à haute température*. France: UJF/INPG - Grenoble; 1975.
10. Rocabois P, Chatillon C, Bernard C. Thermodynamics of the Si–C system I. Mass spectrometric studies of the condensed phase at high temperature. *High Temp High Press* 1995/1996;**27/28**:3–23.
11. Ghosh A, St-Pierre GR. Ternary phase diagrams for the Si–C–O system. *Trans Met Soc AIME* 1969;**245**:2106–8.
12. Pampuch R, Ptak W, Jonas S, Stoch J. Formation of ternary Si–O–C phase(s) during oxidation of SiC. *Mater Sci Monogr* 1980;**6**:435–48.
13. Porte L, Sartre A. Evidence for a silicon oxycarbide phase in the Nicalon silicon carbide fiber. *J Mater Sci* 1989;**24**:271–5.
14. Nagamori M, Boivin J-A, Claveau A. Thermodynamic stability of silicon oxycarbide $Si_5C_6O_2$ (Nicalon). *J Mater Sci* 1995;**30**:5449–56.
15. Vargas T, Navrotsky A, Moats JL, Poly F, Mueller K, Saha A, et al. Thermodynamically stable $Si_xC_yO_z$ polymer-like amorphous ceramics. *J Am Ceram Soc* 2007;**90**:3213–9.
16. Rocabois P, Chatillon C, Bernard C. Vapour pressure and evaporation coefficients of SiO(Amorphous) and SiO_2(s) + Si(s) mixtures by the multiple Knudsen cell mass spectrometric method. *Rev Int Hautes Temp Refract Fr* 1992/1993;**28**:37–48.
17. Rocabois P, Chatillon C, Bernard C. Mass spectrometry experimental investigation and thermodynamic calculation of the Si–C–O system and $Si_xC_yO_z$ fibre stability. In: Naslain R, Lamon J, Doumeingts D, editors. *High temp. ceramic matrix composites*. Abington, Cambridge CB16AH, UK: Woodhead Pub. Ltd., Abington Hall; 1993. p. 93–100.
18. Rocabois P, Chatillon C, Bernard C. High temperature analysis of the thermal degradation of silicon-based materials. II: ternary Si–C–O, Si–N–O and Si–C–N compounds. *High Temp High Press* 1999;**31**:433–54.
19. Chatillon C, Rocabois C, Bernard C. Mass spectrometric study of retarded vaporization of silicon based fibres: origin of their thermal stability. *Key Eng Mater* 1997;**132–136**:1954–7.
20. Sundman B, Jansson B, Andersson JO. The thermo-calc databank system. *Calphad* 1985;**9**:153–90.
21. Cheynet B, Chevalier P-Y, Fischer E. Thermosuite. *Calphad* 2002;**26**:167–74.
22. Bale CW, Chartrand P, Degtesov SA, Eriksson G, Hack K, Mahfoud RB, et al. FactSage thermochemical software and databases. *Calphad* 2002;**26**:189–228.
23. Heyrman M, Chatillon C, Barat C, Fargeas S. Thermodynamique des phénomènes de vaporisation et de condensation dans les fours de coulée de superalliages sous vide. *La Revue de Métallurgie-CIT/Science et Génie des Matériaux* 2003:141–56.
24. Heyrman M, Chatillon C, Pisch A. Congruent vaporization properties as a tool for critical assessment of thermodynamic data. The case of gaseous molecules in the La–O and Y–O systems. *Comp Coupling Phase Diag Thermochem* 2004;**28**:49–63.
25. Chase MW. NIST-JANAF thermochemical tables. J Phys Chem Ref Data 1998;Monograph 9.
26. Meloni G, Schmude RW, Gingerich KA. Knudesn effusion mass spectrometric study of the group IV atomic clusters. In: Hilpert K, Froben FW, Singheiser L, editors. *High temperature materials chemistry*. Germany: Forschungszentrum Jülich; 2000. p. 505–8.
27. Ran Q, Schmude RW, Miller M, Gingerich KA. Mass spectrometric investigation of the thermodynamic properties of the Si_5 molecule. *Chem Phys Lett* 1994;**230**:337–42.
28. Rocabois P, Chatillon C, Bernard C. Thermodynamics of the Si–C system II. Mass spectrometric determination of the enthalpies of formation of molecules in the gas phase. *High Temp High Press* 1995/1996;**27/28**:25–39.
29. Schmude RW, Gingerich KA. Thermodynamic study of small silicon carbide clusters with a mass spectrometer. *J Phys Chem A* 1997;**101**:2610–3.
30. Schmude RW, Ran Q, Gingerich KA, Atomization Enthalpy. Enthalpy of formation of gaseous Si_4 from mass spectrometric measurements. *J Chem Phys* 1993;**99**:7998–8004.
31. Schmude RW, Ran Q, Gingerich KA, Atomization enthalpy and enthalpy of formation of gaseous Si_2 and Si_3 from mass spectrometric measurements. *J Chem Phys* 1995;**102**:2574–9.
32. Muehlhoff L, Choyke WJ, Bozack MJ, Yates JT. Comparative electron spectroscopic studies of surface segregation on SiC(0001) and SiC(000-1). *J Appl Phys* 1986;**60**:2842–53.
33. Behrens RG, Rinehart GH. Vaporization thermodynamics and kinetics of hexagonal silicon carbide. In: Hastie JW, editor. *Characterization of high temperature vapors and gases*. Gaithersburg, Maryland: Nat. Inst. for Standards and Technol; 1979. p. 125–42.
34. Nickel KG, Lukas HL, Petzow G. High temperature corrosion of sic in hydrogen-oxygen environments. In: Hack K, editor. *The SGTE case book – thermodynamics at work*. Cambridge, UK: Woodhead Publishing Limited; 2008. p. 200–11.
35. Birnie DP. A model of silicon self-diffusion in silicon carbide: anti-site defect motion. *Amer Ceram Soc Commum* 1986;**69**:c33–5.
36. Birnie DP, Kingery WD. The limit of non-stoichiometry in silicon carbide. *J Mater Sci* 1990;**25**:2827–34.
37. Jacobson NS, Opila EJ. Thermodynamics of the Si–C–O system. *Met Trans* 1993;**24**:1212–4.
38. Prigogine I, Defay R. *Chemical thermodynamics*. London, UK: Longman; 1967.
39. Banon S, Chatillon C, Allibert M. Investigation of the evaporation thermodynamics and stationnary states (so-called "congruent states") in the study of oxides and their mixtures by the effusion method. Application to Al_2O_3, CaO and the mixtures Al_2O_3–CaO and Ti_2O_3–TiO_2. *High Temp Sci* 1982;**15**:129–49.
40. Malheiros LF, Chatillon C, Allibert M. Congruent vaporisation calculations and differential mass-spectrometric measurement in the study of oxyde mixtures: the Na20-P205 system. *High Temp High Press* 1988;**20**: 361–78.
41. Kreigesmann J, Jodlauk J. Characterizing the consolidation of bimodally distributed fine grained silicon carbide powders. *cfi/Ber DKG* 2002;**79**:37–44.
42. Kreigesmann J, Kraus M, Gros A. Gefügeausbildung von rekristallisiertem SiC. *cfi/Ber DKG* 1998;**75**:83–8.